Arctic and Alpine Research, Vol. 30, No. 3, 1998, pp. 207–221

Prediction of Vegetation Patterns at the Limits of Plant Life: A New View of the Alpine-Nival Ecotone

Michael Gottfried, Harald Pauli, and Georg Grabherr

Department of Vegetation Ecology and Nature Conservation, Institute of Plant Physiology, University of Vienna, Althanstraße 14, A-1091 Vienna, Austria.
gottf@pflaphy.pph.univie.ac.at

Abstract

The distribution pattern of individual plant species, as well as of plant communities, at the transition between the alpine and the nival environment (= alpine-nival ecotone) is likely to be drastically affected by climate change. Currently, the best way to explore the vegetation structure and to detect possible changes is the application of spatial modeling to predict vegetation patterns over larger areas combined with dynamic modeling techniques. Schrankogel in Tyrol, Austria, was selected as a typical high alpine mountain to establish and test such models. As a first step, the predictive model for the spatial pattern of species and plant communities is presented here. Direct and indirect gradient analyses (CA, CCA) were combined with GIS-techniques based on a fine-grained Digital Elevation Model (DEM; pixel size: 1 m^2). Approximately 1000 field samples (vascular plant species and cover within 1 m^2 squares) distributed over the alpine-nival ecotone of the mountain were taken as the vegetation data input. Topographic descriptors were derived from the DEM as habitat characters of those samples. Using the correlations between vegetation samples and habitat characters, single plant species as well as community distribution could be predicted for the pixels of the whole model area (the studied ecotone area contained a total of 650,000 pixels) for which habitat characters were known from the DEM. Distinct distribution patterns at different spatial resolutions appeared for individual species, species groups, and communities in relation to the relief. Descriptors of relief curvature and roughness explained more of the variability than "classical" terrain attributes, such as elevation or exposure. Nevertheless, the altitudinal gradient was clearly reflected by the CCA ordination. As species richness of vascular plants was recorded in each sample plot, biodiversity distribution patterns could be modeled. These patterns showed the general trend of decline of biodiversity with altitude, but with a maximum of species richness at the ecotone itself. Since the relief modifies the high mountain climate remarkably, this differentiated relief dependency of vegetation supports the view that this type of environments will be affected significantly by climate change.

Introduction

If human impact on climate continues as today, a global warming of 1 to 3.5°C is to be expected by the year 2100 (Houghton et al., 1996), leading to temperatures similar to those of the middle Holocene (Beniston, 1994). However, the transition from the ice age to this warm period took place over approximately 50 centuries. A rapid temperature change comparable to the current predictions is only known from the Younger Dryas period when the warming trend at the ending ice age reversed for 200 to 500 yr (Beniston, 1994). Temperature measurements in the Alps, going back to the end of the 18th century (Böhm, 1993), show, with some fluctuations, a warming tendency since 1890. At Sonnblick (3106 m, Austria) the annual mean air temperature increased by 1°C (Auer et al., 1993) during that period. As temperature is a key factor for high mountain plants (for details see Larcher, 1994; Körner and Larcher, 1988; Körner, 1995a) an upward migration of species must be the consequence (e.g., Peters and Darling, 1985; Ozenda and Borel, 1991). In fact, such a trend was demonstrated by comparing present and historical records of 30 alpine summits. Species richness increased remarkably during the last decades at 70% of the investigated mountains (Gottfried et al., 1994; Grabherr et al., 1994, 1995; Pauli et al., 1996). At lower summits the increase was partially due to the invasion of plant species from the alpine belt. This indicates that the transition zone between the alpine belt and the uppermost zone, which is usually termed nival zone (Ozenda, 1985; Walter, 1985; Grabherr, 1995), must be an environment especially sensitive to climate change and, therefore, of high indicative value. Closed alpine swards reach their upper limits there and disintegrate into fragments (Reisigl and Pitschmann, 1958). The organic soil layer gets shallow and finally disappears. The plant cover decreases from more than 50% to less than 5%. Species richness may decrease by more than half over 150 m. The pronounced modification of climatic factors by the microrelief results in a fine-grained vegetation mosaic which may display vegetation changes in various ways.

To take advantage of these characteristics, we started a long-term project to monitor vegetation changes at the alpine-nival ecotone of Schrankogel, Tyrol, Austria. This mountain is situated in a region where ecological research activities have a

0004-0851/98 $7.00

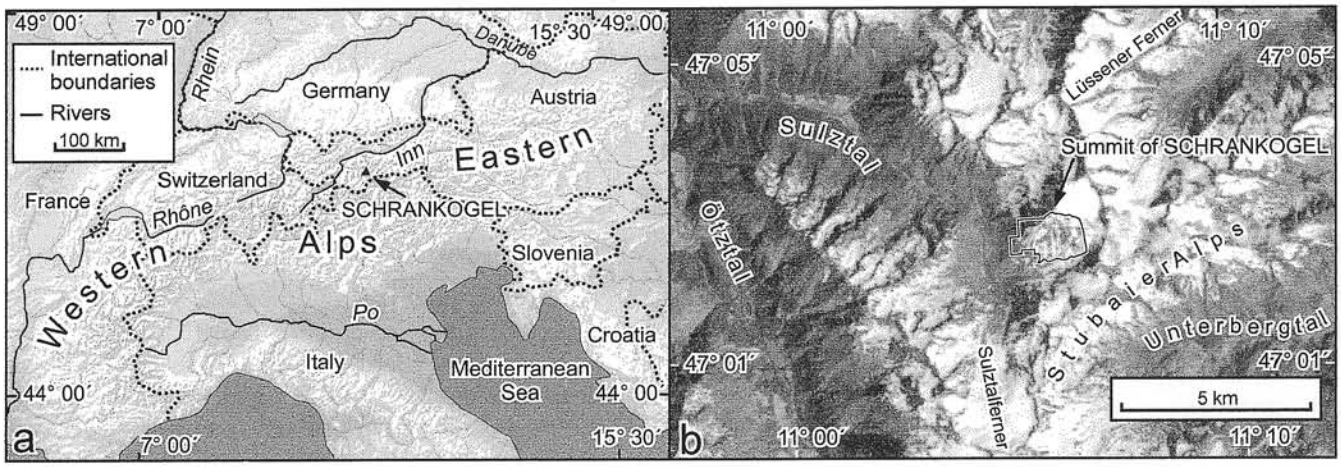

FIGURE 1. The position of Schrankogel (11°05′58″E, 47°02′41″N; 3497 m). a: The chain of the European Alps. b: Satellite image of the heavy glaciated vicinity of Schrankogel in the Stubaier Alps, Tyrol, Austria. Thin line: boundary of the Digital Elevation Model (see Fig. 2a).

long tradition (Moser, 1973; Moser et al., 1978). As a first step, we established a network of permanent plots (started in summer 1994) that were documented in a detailed manner (Pauli et al., 1998). This was followed by the development of a spatially explicit model to predict the distribution of single vascular plant species, as well as communities, for the whole research area using data sets derived from the permanent plots. On the basis of the hypothesis that at least the fine-scale pattern of plant and community distribution is closely related to the relief, we used topographic descriptors derived from a fine-grained Digital Elevation Model (DEM; pixel size 1 m^2) for exploring this relationship. This model, as well as the modeling results, are presented here. Our approach attempts to combine techniques of a Geographical Information System (GIS) as a preprocessing tool for spatial analysis with Canonical Correspondence Analysis (ter Braak, 1986) as the prediction method and uses GIS again as an extrapolation machine and visualization platform. The methodology developed here serves as a tool to create distribution maps of the whole area (first examples are presented here), as well as to explore migration pathways for individual plants.

In a third step we plan to relate the topographic descriptors to climatic characters (mainly temperature) derived from direct measurements in the field as the input for predicting direct effects of climate change.

Methods

APPLICATION OF PREDICTIVE GLOBAL CHANGE MODELING TO THE HIGH ALPINE ENVIRONMENT

Various attempts exist to model vegetation responses and feedbacks to climate (see Martin, 1993, for a classification). Pioneered by Schimper (1898), predictive phytogeographical modeling was developed by Holdridge (1947) and Box (1981), among others, and boomed when the global change discussion came up (e.g., Emanuel et al., 1985; Prentice et al., 1989; Leemans, 1989; Adams et al., 1990; Lenihan, 1993; Cramer and Leemans, 1993; Brzeziecki et al., 1993, 1995; Austin et al., 1994b; Beerling et al., 1995). These spatially explicit models use correlation techniques and are static in the sense that they consider vegetation to be in an equilibrium state with climate (Monserud and Leemans, 1992). Mechanistic, dynamic modeling, on the other hand, attempts to reflect the underlying relationships of components of a system (Mitchell, 1994), often combining basic plant physiology processes to simulate vegetation responses to environmental change (e.g., Woodward et al., 1995) and explicitly addressing temporal characteristics. Developed first for forest systems (e.g., Botkin et al., 1972; Shugart, 1984; Pastor and Post, 1985; Prentice, 1986; Kienast, 1987; Bonan and Korzuhin, 1989; Bugmann and Fischlin, 1992; Botkin, 1993), principles of these so-called gap models were extended to mixed life-forms in forests (Burton and Urban, 1989; Fulton, 1993), to heathlands (Prentice et al., 1987), grasslands (Coffin and Lauenroth, 1990), and recently to alpine plant communities (Humphries et al., 1996).

Dynamic approaches tend to operate, as a result of their mechanistic structure, on spatial scales relevant to the individual species they model. Forest gap models use plots of 100 m^2 to 1000 m^2, while Humphries et al. (1996) modeled alpine plant species on plots of 0.09 m^2. This contrasts with static predictive modeling which came from a global view and often used grid increments on the order of magnitude of one geographical degree since global climate data were only available on this scale (e.g., the IIASA climate database, with a grid resolution of 0.5°; Leemans and Cramer, 1990). This resolution is commonly considered as meeting the requirements of biome modeling, but mountain systems are not well represented in such models. In a 0.5°-grid the chain of the Alps would be 3 to 4 pixels wide. When scaling down, empirical modeling soon meets problems with the availability of climatic data with sufficient resolution. Despite all efforts of climatic downscaling, the "true climate" experienced by alpine plants cannot be predicted from meteorological data due to their strong exposure and radiation-controlled microenvironments (Körner, 1995b).

To consider both the spatial and the temporal nature of the responses of vegetation to environmental change, it was suggested to combine static and dynamic modeling approaches (Monserud and Leemans, 1992). Austin et al. (1994a) pointed out that dynamic modeling of species response over time at a regional level will require input from models of species distribution patterns. This clearly necessitates a harmonization of the spatial scales of these two modeling schemes. The static predictive distribution model presented here attempts to meet the scale requirements of dynamical modeling, providing resolutions in the magnitude of high alpine vegetation mosaics, i.e., of square meters.

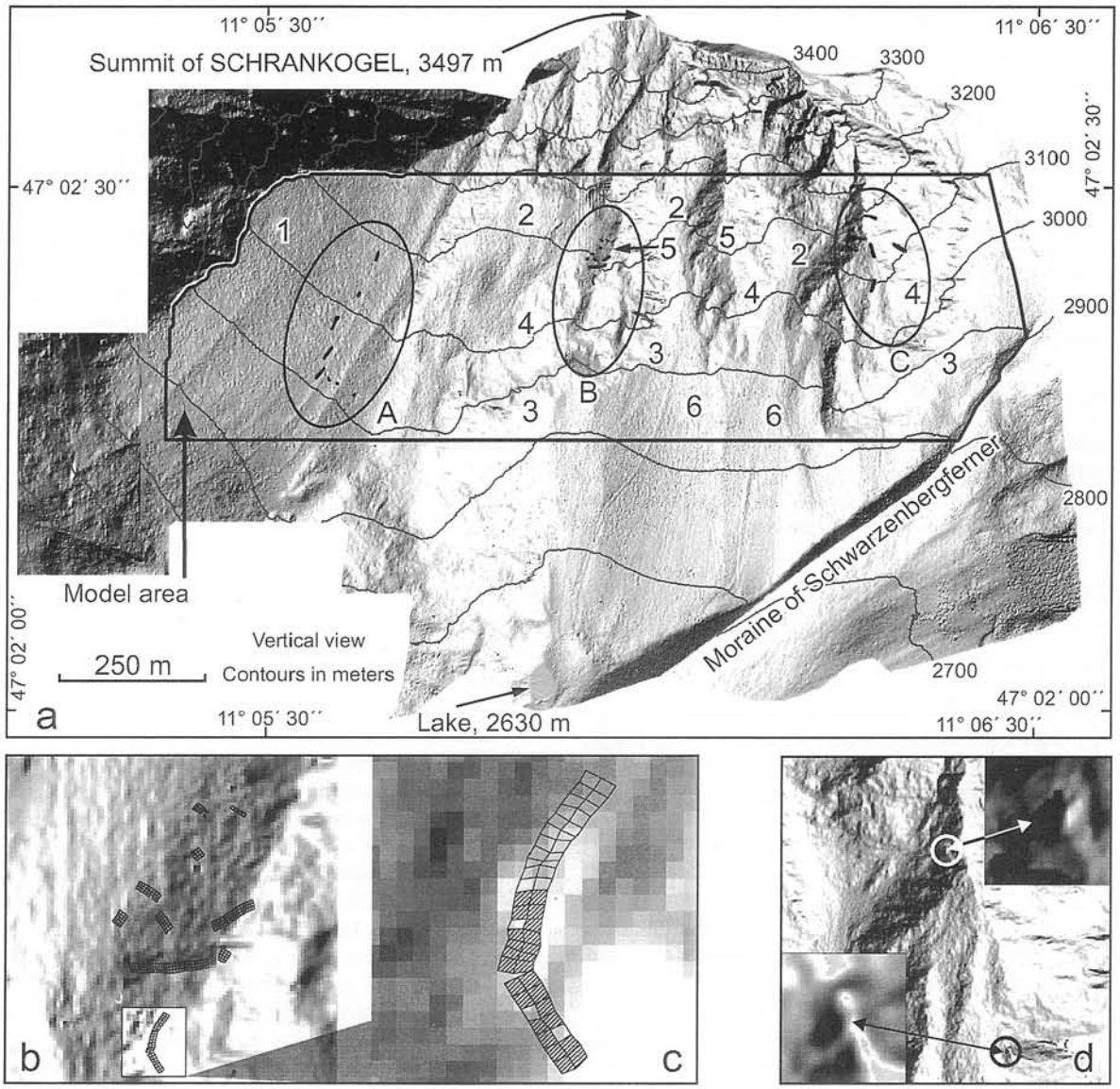

*FIGURE 2. a: The model area and its vicinity. Vertical view of the Digital Elevation Model (DEM). The pixel size of the DEM is 1 × 1 m. Sites of permanent plots: A—southwest slope, B—south ridge, C—southeast ridge. The exact location of the permanent plots in areas A–C is marked by black dots. Types of important topographic situations: 1—well pronounced, southwest slope, rich in scree; 2—hollows with scree; 3—downslope areas below major ridges which structure the main slope; 4—upslope areas on major ridges; 5—ridge tops; 6—wide debris cones below major ridges. b: Zoom into the south ridge (area B in Fig. 2a); permanent plots of 1 × 1 m each, arranged in transects (arrays of plots) of varying length. c: Magnification of the boxed area in Figure 2b. As an example of the biotic information content, the presence of one of the sampled species (*Carex curvula*) in a plot is indicated by hatching. d: Micro- versus macrorelief. Zoom into the southeast ridge (area C in Fig. 2a). White circle: a west-exposed, shady location of few square meters (dark), embedded in a southwest-exposed slope. Black circle: a similar west exposed location, embedded in a southeast-exposed slope (for explanations see text).*

INVESTIGATION AND MODEL AREA

Schrankogel (3497 m a.s.l., Tyrol, Austria; Fig. 1) was selected as a high siliceous mountain typical for the Eastern Central Alps. Surrounded by wide glaciers (Fig. 1b) it offers a mosaic of ridges and steep slopes with several exposures (i.e., compass directions) which bear swards or screes and which vary with moderate steep or gentle hollows, where snow persists often far into the summertime (for snow accumulation phenomenons, see Barry, 1992). The investigation area contains three main sites (Fig. 2a): On the southwest ridge and slope (A) the closed alpine sward (*Caricetum curvulae*) disintegrates at around 2900 m into sward fragments and finally is replaced by nival scree vegetation. At the south ridge (B) the sward reaches its limits at about 3050 m, and at the southeast ridge (C) at 3150 m. The transition zone, from typical swards to typical nival scree vegetation, is approximately 100 altitudinal meters high and 40° steep. This alpine-nival ecotone shows local deviations and a slight inclination in the altitudinal position of the transition zone from west to south to east, which reflects the mesoclimatical situation of the region in a typical manner. The model area is about 400 altitudinal meters high (2800–3200 m, 650,000 m^2; Fig. 2a).

SAMPLING DESIGN

About 1000 single permanent plots of 1 × 1 m, constructed of flexible measuring-tapes, were installed in the field. The corners of each plot were exactly geo-positioned. The plots were arranged in transects (long arrays of plots) of 3 m (sometimes 2 m) width and 3 up to 30 m length (Fig. 2b–c). The single plot size of 1 m^2 was chosen for two reasons. First, due to the narrow mosaic of environmental conditions changing over short distances, the vegetation patterns at the ecotone are extremely small-scaled. The chosen size fits the requirements of the minimum area approach (Braun-Blanquet, 1964). Second, the plots were designed to detect migration effects and, hence, according to the slow migration rates of alpine plants (Grabherr et al., 1995), had to be small and placed near to each other.

Due to practical constraints like accessibility, danger of rockfall, and cost effectiveness, the transects could not be randomly positioned within the research area, but were selected subjectively, somewhat grouped together (Fig. 2a, A–C), but covering as much terrain situations as possible.

VEGETATION DATA SET

Two biotic data categories were used in this study: (1) a list of vascular plants of each plot with their abundances (measured in the field as the visually determined percentage of the surface of the total plot area covered by the species; the abundance values were log-transformed and divided by the maximum value of the respective species), and (2) the result of a TWINSPAN-classification (Hill, 1979) of each plot into several community types.

ABIOTIC DATA SET

The abiotic data set was derived from a Digital Elevation Model (DEM) with a pixel size of 1 × 1 m, matching the size of the permanent plots. It covers nearly 1,700,000 m^2 between 2470 and 3497 m a.s.l., which, according to our knowledge, makes it the DEM with the highest resolution of such an area, which was produced for a part of a mountain system (Fig. 2a). The plots sampled in the field were linked to the DEM by triangulation. All derivations based on the DEM, as well as all subsequent spatial explicit modeling steps, were performed with the Geographical Information System ARC/INFO (ESRI, 1995).

From the DEM a variety of topographic descriptors were computed. Aside from the traditional derivatives slope and aspect (exposure), a number of more sophisticated descriptor types were extracted (Table 1). Each descriptor was represented by a separate grid layer which was computed by moving a window of 3*3 cells in a stepwise manner over the entire DEM layer. After fitting a polynomial function to the 9 cells of the window, the descriptor's value was calculated based on the coefficients of the fitted polynomial and stored in the interior cell of the moving window (see Moore et al., 1991, for a description of related techniques and equations).

Some of these descriptor types can be easily explained verbally, while others cannot. For example, RVII, which was found more or less by chance, lacks a tight verbal interpretation, but revealed high correlation values with vegetation patterns. This is no severe drawback, since this explorative study was aimed foremost at obtaining good modeling results.

The differences of climatic features on different scales, referred to as micro-, meso-, and macroclimate, are well known. Especially when dealing with ecological implications of topography, the question of appropriate scaling must be taken into account as well. Mountain ecologists know that the relief has different effects on species distribution on different spatial scales. For instance, a west-exposed point embedded in a larger, southeast-exposed slope area will, in most cases, not show the same vegetation as a similar west-exposed point in a southwest-exposed slope area. Both, the fine-scaled, as well as the wider scaled exposure situation, influence the vegetation pattern. This is what could be labeled as micro-, meso-, and macroscale of exposure (Fig. 2d). Such effects also hold true for other topographic features, e.g., steepness. A small flat place embedded in a flat slope is not impacted by rockfall, whereas vegetation on a flat site in a very steep slope is extremely endangered by falling stones.

To incorporate such effects into the analysis, each topographic descriptor was smoothed using so-called "focalfunctions" of ARC/INFO-GRID. Each cell in the grid receives the mean (or in some cases the standard deviation, see Table 1) of the surrounding cells delineated by a circle-shaped window of a distinct radius around the center cell by moving this window over the whole grid. The window radius was increased in steps (r = 2, 5, 10, 20, 30, 40, 50, 75, 100 m), with each descriptor type at each resolution generating an extra descriptor layer. These layers were named according to the abbreviations defined in Table 1 and to the radius (e.g., SL-2, EA-50, CII-75). Figure 3 shows four descriptor types on three smoothing levels, forming 12 descriptor layers.

Due to technical constraints in the program, some of these topographic descriptor layers were transformed to coarser resolutions using resampling instead of focalfunctions. In these cases the cell size of the basic elevation layer was increased in steps (compare Fig. 3, CII-5, CII-30, CII-100).

The combination of 17 descriptor types with 10 resolutions, plus altitude (which was not smoothed), supplied 171 different descriptor layers. The values of each descriptor layer were assigned to the center point of each permanent plot by linear interpolation of the values of the four surrounding cells of the respective layer. At this stage two data sets existed, one with the cover value of each species in each sampled plot, and one with the values of each environmental variable in each plot.

ANALYSIS OF RELATIONSHIPS BETWEEN SPECIES DISTRIBUTIONS AND ENVIRONMENT

The core of each spatial predictive model is the analysis of the relationships between the units the distributions of which have to be modeled—in this case the vascular plant species under observation—and the environmental descriptors which are used to perform the prediction—in this case the topographic descriptors. As a rather large number of units has to be treated (19 species, 170 environmental descriptors in the first step), the program package CANOCO (ter Braak, 1988, 1990) was appropriate for this analysis (see Birks et al., 1994, for a bibliography of applications).

Indirect Gradient Analysis

To explore the multidimensional structure of the vegetation data set, an indirect gradient analysis was performed on the species data using Correspondence Analysis (CA). The basic algorithm of this method is weighted averaging (for an introduction see, e.g., ter Braak and Looman, 1995, and ter Braak, 1995), which implies unimodal response curves of species to the environment.

TABLE 1

Topographic descriptor types, extracted from the Digital Elevation Model

Descriptor type	Derivation in the GIS	Linked features/comments	Abbreviation[a]
Altitude	Elevation above sea level	Temperature	ELEV
Slope	Slope	Accumulation of scree and snow (negatively correlated); avalanches; rockfall; irradiation	SL
Easting	East-exposed fraction of aspect (exposure)	Weather events, which are commonly west to east directed in the Eastern Alps (wind-, rainshadow)	EA
Southing[b]	South-exposed fraction of aspect (exposure)	Irradiation	SO
Hillshade	Reflection value when illuminating the DEM from a distinct direction (here: azimuth angle 180° (south), altitude angle (40°)	Irradiation, taking into account slope and aspect	HS
Upslope area	Catchment area above a distinct location; also termed flow accumulation	Distance to ridges: each location on a ridge has value 0, while runoff paths are differentiated (the higher the upslope area, the higher the value); wind; rockfall; scree and snow accumulation; moisture	UA
Inverse upslope area	The DEM is inverted (max(ELEV)−(ELEV)) and flow accumulation (UA) is computed	Distance to runoff paths: each location within a runoff path has value 0, while ridges are differentiated (the more dominant the ridge, the higher the value); similar to UA, but with different numerical properties	IUA
Curvature I[c]	Curvature, i.e., convexity/concavity of the surface	Moisture; accumulation of snow and scree in hollows (negatively correlated)	CI
Curvature II[c]	Profile curvature, i.e., curvature of the surface in the direction of slope	Influences acceleration and deceleration of flow, and therefore erosion, deposition, rockfall, and moisture	CII
Curvature III[b,c]	Planform curvature, i.e., curvature of the surface perpendicular to the slope direction	Influences convergence and divergence of flow; similar to CI and CII, but with different numerical properties	CIII
Curvature IV	Mean of CIII in a distinct radius around the location; for explanation see text	Distinguishes areas with many little tops or ridges from areas with many little hollows	CIV
Roughness I	Standard deviation of EA in a distinct radius around the location; for explanation see text	Relief roughness; the more diverse the aspects (exposures) in a certain area, the rougher the relief	RI
Roughness II	Similar to RI, but derived from SO	Compare RI	RII
Roughness III	Similar to RI, but derived from a slope-aspect-index (an index combining slope and aspect parameters, used to produce hillshades)	Compare RI	RIII
Roughness IV	Similar RI, but derived from HS	Compare RI	RIV
Roughness V[b]	Mean of absolute value of CIII within a distinct radius	High values describe areas with many little hollows and/or tops	RV
Roughness VI[b]	Standard deviation of absolute value of CIII within a distinct radius	In areas with high values the variation in depth/height of hollows/tops are high	RVI
Roughness VII	Ratio of RV and RVI	High descriptive value, but verbal interpretation difficult; see text	RVII

[a] Abbreviations also used in Table 3 and Figures 3 and 4.

[b] Descriptors of minor importance in the following analysis, because of being high correlated with other descriptors.

[c] Descriptors which are transformed by resampling instead of smoothed by using focalfunctions (see Fig. 3, and explanations below).

Direct Gradient Analysis

Canonical Correspondence Analysis (CCA; ter Braak, 1986) extends CA to a direct gradient analysis by regressing the species data to environmental variables. For each environmental variable a canonical coefficient—similar to regression coefficients in indirect methods, but with different statistical properties—on each environmental axis is computed by CANOCO. These coefficients were of central importance for the following steps of the model presented here. However, if some of the environmental variables in the input data set are highly correlated with each other, the canonical coefficients became unstable. High correlations between variables in a multiple regression equation are reflected by high Variance Inflation Factors (VIFs, Montgomery and Peck, 1982), which are also listed by CANOCO. To avoid such unstable coefficients, the initial set of 170 environmental variables was iteratively reduced, removing in each step those variables with the highest VIFs. In this way the set of environmental variables was reduced to 37, few enough to avoid collinearity between the variables, but as large as possible so as not to loose any environmental information.

For both the CA and CCA the default options of CANOCO 2.1 were used (see ter Braak, 1988).

SPATIAL EXTRAPOLATION OF DISTRIBUTION PATTERNS

For each sampled permanent plot the position in the multidimensional space of the CCA can be computed. This can be performed in the species space by averaging the weighted species scores of the species occurring in the sample. Alternatively, it can be computed in the environmental space, using the environmental values in the sample weighted by the canonical coefficients of the environmental variables. This multidimensional position can also be computed for each of the 650,000 cells of the modeling area, since the environmental descriptors are available for the whole area. At this stage of the model, the data were exported to GIS again. For each dimension of the CCA ordination space, a separate coordinate layer was computed in ARC/

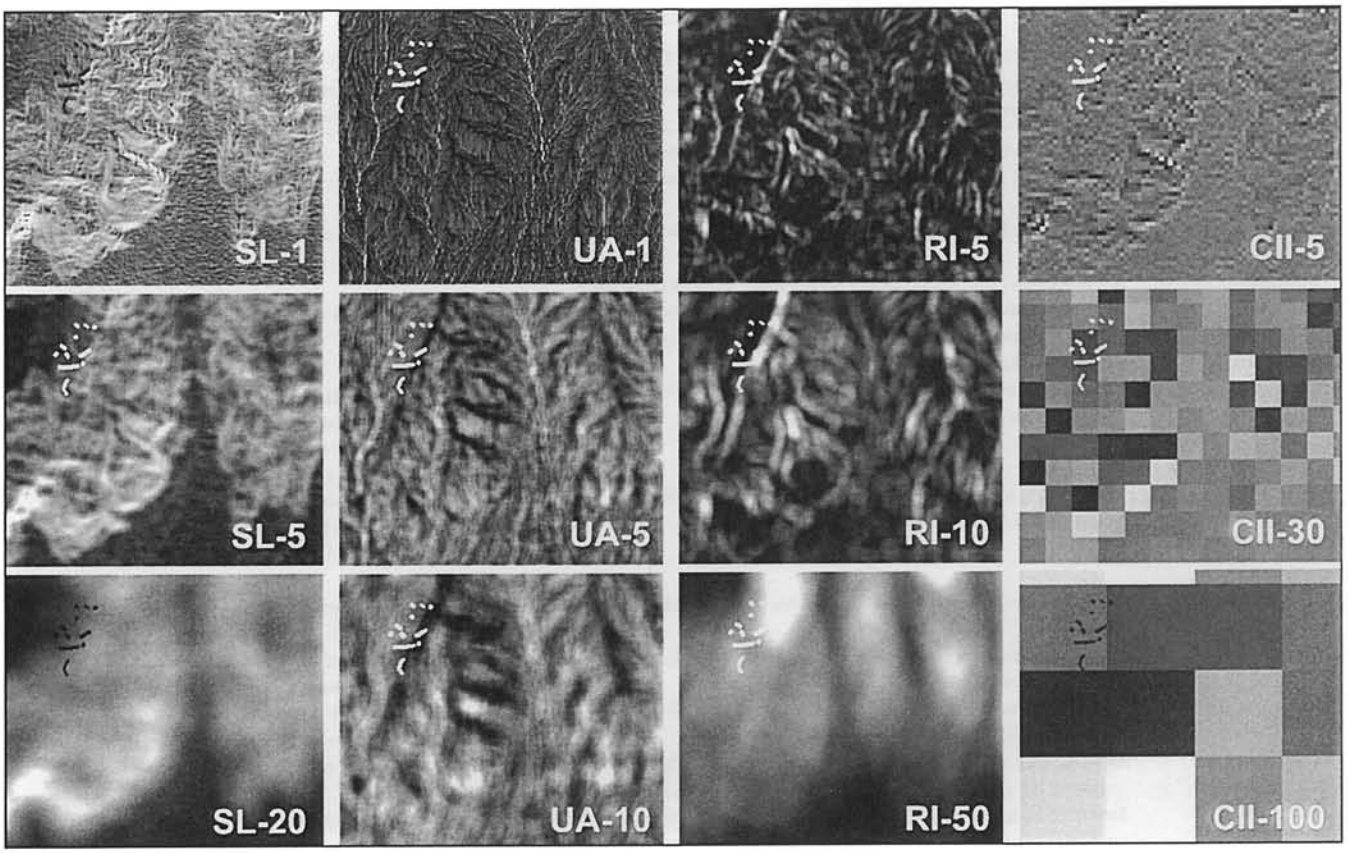

FIGURE 3. Twelve examples of spatial topographic descriptor layers, derived from the DEM (Fig. 2a). Four descriptor types (left to right) on three spatial smoothing levels (top to bottom). Characters indicate the descriptor type, numbers the smoothing level. SL—slope, UA—upslope area, RI—roughness I, CII—curvature II (see also Table 1). Bright pixels: high descriptor values; dark pixels: low descriptor values. SL, UA, and RI were smoothed using focalfunctions, CII was transformed using resampling (for explanations see text). The location of some of the sampled plots (compare Fig. 2a, area B) is marked by white (or black) dots.

INFO-GRID as a linear combination of environmental values weighted by canonical coefficients, similar to what was done earlier for the sampled plots. For each cell the nearest neighbor—the sample with the least Euclidean distance—can be determined. This step (approx. $0.65 * 10^9$ distance calculations in four dimensions) needed about 24 h computation time (on a Sun Sparc 20 workstation). Its output revealed two new layers for the model area. In the first layer to each cell the sample number of its nearest neighbor (that permanent plot of the smallest Euclidean distance in the CCA ordination space) was assigned. The second layer took for each cell this smallest Euclidean distance itself. These values were seen as a measure for the confidence level of the prediction. The closer a real environmental situation exists to the extrapolated position, the more confidence one can have in the prediction results.

Any information which is connected with sample numbers of the plots sampled in the field could now be extrapolated and displayed over the whole model area, as to each cell a distinct sample number was assigned.

The results allowed production of several distribution maps of species, of communities, of ecological indices such as species richness, as well as of technical indices of the prediction scheme (Figs. 5, 6).

MODEL EVALUATION

To evaluate the predictions, about 10% of the plots in the input data set (i.e., approx. 90 plots) were removed. Then the extrapolation was run again, and the resulting predictions for the model cells at the locations of the removed plots were compared to the data sampled in the field. For 21 species (19 of them being input to the CCA, and 2 more, which were of interest for a comparison with the vegetation classification) each presence, as well as each absence, in the sampled set compared to the predicted set, was counted. This led to 2×2-contingency tables with counts for s0p0 (species is absent in sampled plot and in predicted plot), s1p0 (species is present in sampled but absent in predicted plot), s0p1, and s1p1. These counts were set in relation to expected counts (implying that no correlation between sampled set and predicted set exists) which can be computed from the row and column sums of the contingency table. The ratio of expected counts and counts resulted by the prediction model was termed s0p0- and s1p1-performance, and s1p0- and s0p1-failure, respectively. For both types of indices, a random model would produce scores of 100%. The higher the performance-indices score beyond 100%, the better the prediction model works. In turn, for failure-indices the model works the better, the more they go below 100%. As a statistical measure of agreement between sampled and predicted distributions we used the Kappa statistic (Cohen, 1960; Monserud and Leemans, 1992). This index is 0 if the two sets are uncorrelated and reaches 1 if the sets are perfectly correlated.

This procedure (of removing 10% of the plots, performing the extrapolation, comparing sampled and predicted presence/

TABLE 2

Results of indirect (CA) and direct (CCA) gradient analysis

	Ax1	Ax2	Ax3	Ax4	Sum of all eigenvalues
CA					Unconstrained = total inertia
Eigenvalue	0.41	0.21	0.19	0.15	1.796
Cumulative percentage variance of species data explained	22.6	34.3	45.0	53.5	
CCA					Constrained (canonical)
Eigenvalue	0.28	0.11	0.08	0.05	0.676
Species-environment correlation	0.84	0.73	0.66	0.64	
Cumulative percentage variance of species data explained	15.7	21.8	26.4	29.3	
Cum. perc. variance of species-environment relation explained	41.6	57.8	70.1	77.8	

absence of species) was repeated 9 times, and the results for all ten evaluation runs were averaged. Then the 21 species under consideration were ranked according to each of their mean performance/failure-ratios, and Kappa values, respectively, and clustered comparing their ranks in these 5 attributes. This resulted in groups of species that were treated by the prediction model in a similar way.

Results

GRADIENT ANALYSIS

The indirect gradient analysis (CA) showed a length of the first ordination axis of about five standard deviations, indicating a complete turnover of the species composition within the plots along this axis. This supported the implication of unimodal rather than linear response patterns (ter Braak, 1995) in our data set, and, hence, the use of weighted averaging methods.

The first four CA-axes explained 54% of the total variance in the sample scores of the vegetation data set (as indicated by: Cumulative percentage variance of species data explained; Table 2). When switching to direct gradient analysis (CCA), this value dropped to 29% due to the constraints in ordination, i.e., the regression of the sample scores to given environmental variables. This indicated that important environmental variables were not measured, but, in turn, that a considerable part of the species distribution was predictable by the supplied topographic data. Taking into account (1) that vegetation data sets are noisy in general (Gauch, 1982), (2) that high alpine and nival data sets are, according to our experience, even more so, and (3) that only the relief is used to explain this structure, this value is remarkable high. The inertia in the species data dropped to 0.68 in the constrained analysis because the species scores were fitted now to environmental variables. The first four axis carried 78% of this inertia (indicated by: Cumulative percentage variance of species-environment relation explained). This showed that more ordination axes would not enhance the precision of the predictions of the following extrapolation substantially, while each additional axis would increase the computational efforts for the extrapolation considerably.

A Monte Carlo permutation test showed that the species

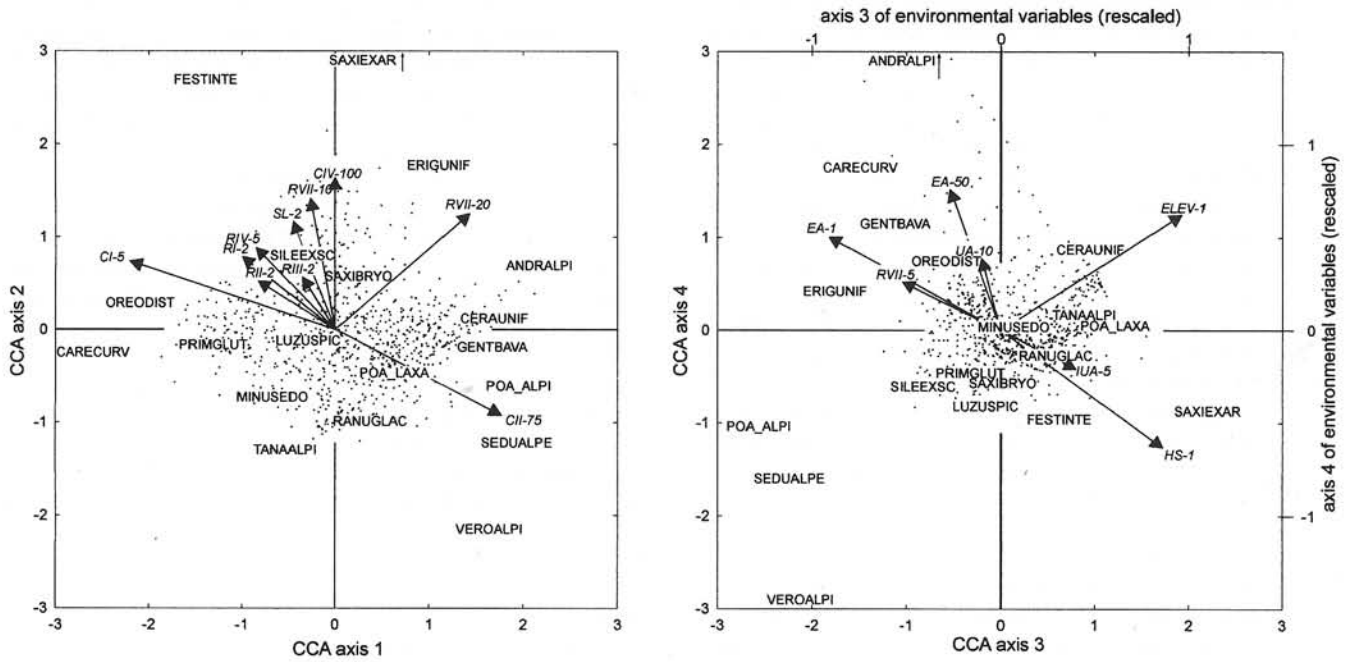

FIGURE 4. Canonical correspondence analysis (CCA) biplots of environmental variables in relation to species on axis 1 vs. 2 and 3 vs. 4. Abbreviations of species names: First four characters of genera plus first four characters of species names. Full names shown in Table 4. For environmental variables (italic) see Table 1. Samples plotted as dots. Lines indicate the direction of maximum variance of environmental variables, arrows point to high values.

TABLE 3

Intra-set correlations[a] of environmental variables with CCA-environmental axis, T-values[a] of the canonical coefficients

	Intra-set correlations with CCA-axis		T-values of canonical coefficients	
Variable	Ax1	Ax2	Ax1	Ax2
CI-5	***−0.52***	0.25	***−3.10***	−1.60
CII-75	***0.44***	−0.31	***11.90***	−4.80
RVII-20	***0.31***	0.43	***8.10***	0.80
CIV-100	0.00	***0.54***	1.60	***10.60***
RVII-10	−0.06	***0.48***	−4.00	***3.00***
SL-2	−0.11	***0.40***	0.80	***2.90***
RIV-5	−0.22	***0.31***	−3.60	***6.20***
RI-2	−0.24	***0.28***	−0.20	***4.10***
RIII-2	−0.09	***0.21***	3.10	***−5.10***
RII-2	−0.18	***0.20***	−0.10	***−3.30***
	Ax3	Ax4	Ax3	Ax4
ELEV-1	***0.34***	0.30	***10.60***	10.90
RVII-5	***−0.20***	0.14	***−4.30***	2.70
IUA-5	***0.18***	−0.10	***3.10***	−5.10
EA-50	−0.10	***0.36***	−5.30	***−2.20***
HS-1	−0.37	***−0.30***	0.70	***−3.70***
EA-1	−0.34	***0.25***	−1.90	***4.80***
UA-10	−0.06	***0.17***	6.70	***6.60***

[a] Values in bold italic were considered for the decision on which axis the variable should be interpreted.

were significantly related to the environmental variables (P = 0.01 for each ordination axis which was displayed).

The two ordination diagrams (Fig. 4) show—for clarity—only the set of the 10 (on axis 1 vs. 2) and 7 (on axis 3 vs. 4) topographic variables which performed best in the analysis. They were selected according to their importance measured by (1) intra-set correlations (the correlations between variables and environmental axes), (2) canonical coefficients (not indicated here), and (3) T-values for these coefficients (Table 3). The intra-set correlations can be obtained by dividing the inter-set correlations, i.e., the correlations between environmental variables and the species axes, by the species-environment correlations. The variables were interpreted on this axis, to which they show a high correlation paired with a reasonably high T-value.

In CCA biplots, the sequence of species response optima along ordination axes as well as environmental variables can be read by drawing lines from the species scores coordinates perpendicular to the axis, or environmental arrow (see ter Braak, 1995). Axis 1 of the biplot reflects mainly a curvature gradient. It shows sward species like *Carex curvula* or *Oreochloa disticha* preferring exposed sites (*CI*) on a relatively narrow scale of 5 m (*CI-5*) while *Androsace alpina* or *Poa alpina* avoid such positions. This is an effect of accumulation of snow and moisture in little hollows, which sward species cannot withstand. *CII,* the profile curvature, is in principle negatively correlated with *CI,* which is also the case for this data set. *CII-75* models large hollows which accumulate scree, inhabited by typical scree species like *Androsace alpina* or *Sedum alpestre.* Axis 2 is correlated with a variety of relief roughness variables (*RI, RII, RIII, RIV, RVII*) on small resolutions, with slope (*SL-2*), and, most strongly, with *CIV* on the 100 m resolution. The ecological knowledge about and field observations of *Saxifraga exarata,* the species most outstanding on axis 2, fit this set of variables which describes rough, steep areas that are well structured by many little ridges or tops.

The environmental axes 3 and 4 are rescaled in the diagram for graphical reasons (the gradients on these axes are, of course, not stronger than those displayed on axis 1 or 2, which would contradict the concept of canonical correspondence analysis). Axis 3 bears mainly the altitudinal gradient (*ELEV-1*), separating species being constrained to the lower parts of the investigation area, such as *Veronica alpina, Sedum alpestre,* or *Poa alpina,* from those species which occur more often and with higher cover values in the higher regions of the model area, such as *Poa laxa, Tanacetum alpinum,* or *Cerastium uniflorum.* Species, which show an indifferent response to altitude in this data set, are plotted near the center of the axis (e.g., *Minuartia sedoides* or *Ranunculus glacialis*). Another variable correlated with axis 3 is *IUA-5,* modeling distances to runoff-paths on a fine resolution; again, the response is strongest by *Saxifraga exarata.* Axis 4 is correlated to exposure variables (*EA*). Note that there is a considerable difference in the response of some species to exposure on different resolution levels. *Carex curvula* needs both, the east-exposure on the microscale, the immediate surrounding (*EA-1*), as well as on the macroscale (*EA-50*), which shows that—at least in the higher parts of the area—only the larger southeast-exposed ridges keep sufficient habitats for this species. On the other hand, e.g., *Sedum alpestre* reacts similarly to *EA-1,* but not to *EA-50.* Also insolation (*HS-1*) and upslope area, or distance to ridges (*UA-10*) have some effects on this axis.

A somewhat obscure role is played by the relief roughness variable RVII. It occurs with considerable correlations on axis 1 (*RVII-20*), axis 2 (*RVII-10*) and axis 3 (*RVII-5*), despite the fact that it lacks a clear verbal explanation, as mentioned earlier.

SPATIAL EXTRAPOLATION

Figure 5 displays the predicted distribution patterns of eight species which represent typical patterns of distributions (for topographic details and numbers mentioned below see Fig. 2a). *Androsace alpina* (Primulaceae; Fig. 5, top) is a common species in the modeled area; though it is also frequent in its lower parts, it is found with higher abundances at higher altitudes. It prefers scree areas, such as the pronounced southwest slope (1) and the wide hollows (2) of the area. It also inhabits downslope stands below major ridges (3), but avoids situations near or on the top of these ridges (4, 5). On the latter habitats, competition by sward species is high, as expressed by the pattern of *Carex curvula* (Cyperaceae; Fig. 5, bottom). This keystone species of the alpine swards keeps away from habitats with too much environmental pressure by snow, scree, or rockfall, and, therefore, prefers the safest sites in the area, which are the southeast-exposed, midslope situations below the major ridges (4). *Oreochloa disticha* (Poaceae; Fig. 5, center left) copies that pattern, but is more abundant at the tops of ridges, being better adapted to wind, according to its role as a sward pioneer species. *Silene exscapa* (Caryophylaceae; Fig. 5, center left), which has its optimum at the upper limit of pioneer swards, is also most abundant in these habitats, protected from excessive erosion, but reaches deep into the scree areas, thereby linking the alpine with the nival zone. A number of species, e.g., *Poa laxa* (Poaceae; Fig. 5, center left), are widespread in the upper alpine, as well as in the nival zone. They do not show distribution preferences in the model area, either in presence or in abundance. This is not the case for another grass, *Poa alpina* (Fig. 5, center right), which shows a strong dependence on the altitude. It inhabits the lower parts of the area which are rich in scree (1, 3, 6). *Sedum alpestre* (Crassulaceae; Fig. 5, center right) behaves similarly to *P. alpina* re-

garding its presence/absence, but differently concerning its abundance patterns. While *P. alpina* is highly abundant (magenta pixels) on some southeast-exposed, downslope situations (3) and inhabits the wide scree cones below (6) regularly, though in a scattered manner (cyan pixels), the opposite is the case for *S. alpestre,* which shows its highest abundances (magenta and yellow pixels) at the most erosive habitats in the area (6). *Saxifraga oppositifolia* (Saxifragaceae; Fig. 5 center right) is an example for those sparse species in the data set that were not taken into account for the CCA, but which, nevertheless, can be extrapolated over the model area since whole vegetation samples with all their species information and not just individual species are extrapolated. The scattered distribution of this species, with higher abundances restricted very narrowly to ridges, corresponds well with field observations in the investigation area.

One cannot overlook conspicuous rectangular structures in the predicted distribution patterns, varying in size and density, from area to area, and from species to species. Some of the terrain curvature descriptors were not smoothed to lower resolutions in a continuous way, but by enhancing the cell sizes of the descriptor layer (compare Fig. 3 CII-5, CII-30, CII-100). This influences the extrapolation. Some species are more strongly related to such descriptors, while others are not. For instance CII-75 overwhelms the prediction of *Androsace alpina* (represented by the cyan squares in Fig. 5—*A. alpina,* with 75 m edge length). This relations vary also among different parts of the model area. On the broad southwest exposed slope, where terrain curvature—at least on coarser scales—does not change over wide areas, such descriptors are not important.

The Schrankogel vegetation data set was also floristically classified, revealing a number of distinct units, e.g., nival vascular plant assemblage, scattered single vascular plants in the nival/subnival zone, pioneer sward vegetation with *Carex curvula,* and scattered cushion plant assemblage of the type *Androsacetum alpinae* (details of these analysis will be published elsewhere). As was the case for individual species, these vegetation types can be extrapolated to the model area since each cell of the model can be linked—via its assigned sample number—to a certain vegetation type. In Figure 6a, the several vegetation types were grouped into three important formations. The alpine swards and pioneer sward vegetation (cyan) has its uppermost closed stands on the lower parts of the southwest slope, and its pioneer stands on the major ridges of the south slope. Widespread on the lower parts of the area which are rich in scree is what can be assigned to the already syntaxonomically described type of siliceous high alpine and nival scree vegetation, the *Androsacetum alpinae* s. l. (yellow). Note that—surprisingly on first glance, but reasonably due to the relief conditions—the swards extend on favorable stands far beyond the main distribution area of this type. Above the *Androsacetum,* some vegetation types, grouped together as nival and subnival vegetation (magenta), lead to the true nival zone. The transition from the upper alpine to the nival zone is clearly displayed. Figure 6b–e show some single vegetation types. The true nival vegetation, consisting of only five vascular plants, provisional termed nival vascular plant assemblage is closely restricted to the high parts of the model area (Fig. 6b). At the stands which face the highest environmental pressure from scree and snow, i.e., the shady, gorgelike hollows in the upper parts of the south slope, the model predicts a vegetation which has no stable species composition but consist only of one or the other nival species at random (scattered single vascular plants in the nival/subnival zone, Fig. 6c). The ecological limits of vascular plant life are reached here. In turn, closed and pioneer swards with *Carex curvula* are predicted only on the favorable, southeast-exposed, solid parts of the slopes (Fig. 6d). Figure 6e displays the extrapolation for the core association of siliceous high alpine screes, the *Androsacetum alpinae.*

Figure 6f–h show three different thematic maps. In Figure 6f the percentage of surface covered by vascular plants is displayed, and in Figure 6h the species richness. Note that the altitudinal decline in species richness is predicted not only related to changes in vegetation types, but also within the types themselves. This can be judged by comparing Figure 6a, where the sward and pioneer sward vegetation captures a wide altitudinal range, with Figure 6h, which makes clear the decreasing species richness. However, the general trend of decreasing biodiversity with altitude is superceded by a tendency of maximum species richness at the ecotone itself. One can inspect that best in the left part of Figure 6h, the southwest-exposed, well pronounced slope (compare Fig. 2a). This slope shows medium species richness (yellow) in the area below 2900 m, low species richness (cyan) above 3000 m, and a peak of species richness (magenta) between 2900 and 3000 m (for altitudes compare contours in Fig. 2a).

Figure 6g does not display any vegetation, but a measurement for the goodness of the prediction (confidence level of prediction). Magenta cells have a short Euclidean distance to the next sampled plot in the multidimensional environmental CCA space used for the extrapolation. The topographic situation of such a cell is, therefore, considered as satisfactorily comparable to a situation sampled in the field. Cyan cells, in turn, have their next neighbor in the CCA space relatively far away and are considered as more weakly comparable to the sampled data.

MODEL EVALUATION

The predictive power of the model differed for the species studied; this is summarized in Table 4. The values presented in this table have to be interpreted as in the following example: e.g., *Carex curvula,* present in 14.3 (referred to as s1-cases) of the plots (n = 92, average over 10 runs) which were randomly selected out of the total 903 plots sampled in the field, was predicted by the model to be absent with 109% of the accuracy which would be expected by chance (s0p0-performance). The number of plots where absence was sampled and presence was predicted (s0p1-failure) was only 38% of what would have been expected for a random distribution. The s1p0-failure, to be interpreted analogously, was 49%. The number of cells, where *C. curvula* was present, both in the field and in the model prediction, exceeded more than 4 times the random prediction (s1p1-performance = 477%). Kappa (0.55) was quite high, indicating a good agreement between reality and prediction.

Clustering the species according to the prediction indices of Table 4 revealed five meaningful groups. The prediction performed best for the species of group 1. Taking into account that these species were present in comparably few sampled plots (less than 20% on average: s1-cases = 16.6 out of 92), all predictions agreed quite well with reality (Kappa = 0.48). Sampled presences were confirmed by the prediction more than three times beyond random (s1p1-performance = 337%). These species have well-defined topographic niches (see displays for *C. curvula, P. alpina,* and *S. alpestre* in Fig. 5). This does not mean necessarily that they have similar distribution patterns, or ecological niches, but that their distributions are easy to interpret according to terrain conditions. Group 2 contained species with similar Kappa values. Due to more s1-cases, the predictive power dropped to 171% of a random performance. Group 3—species showed again better s1p1-performances, but due to high predic-

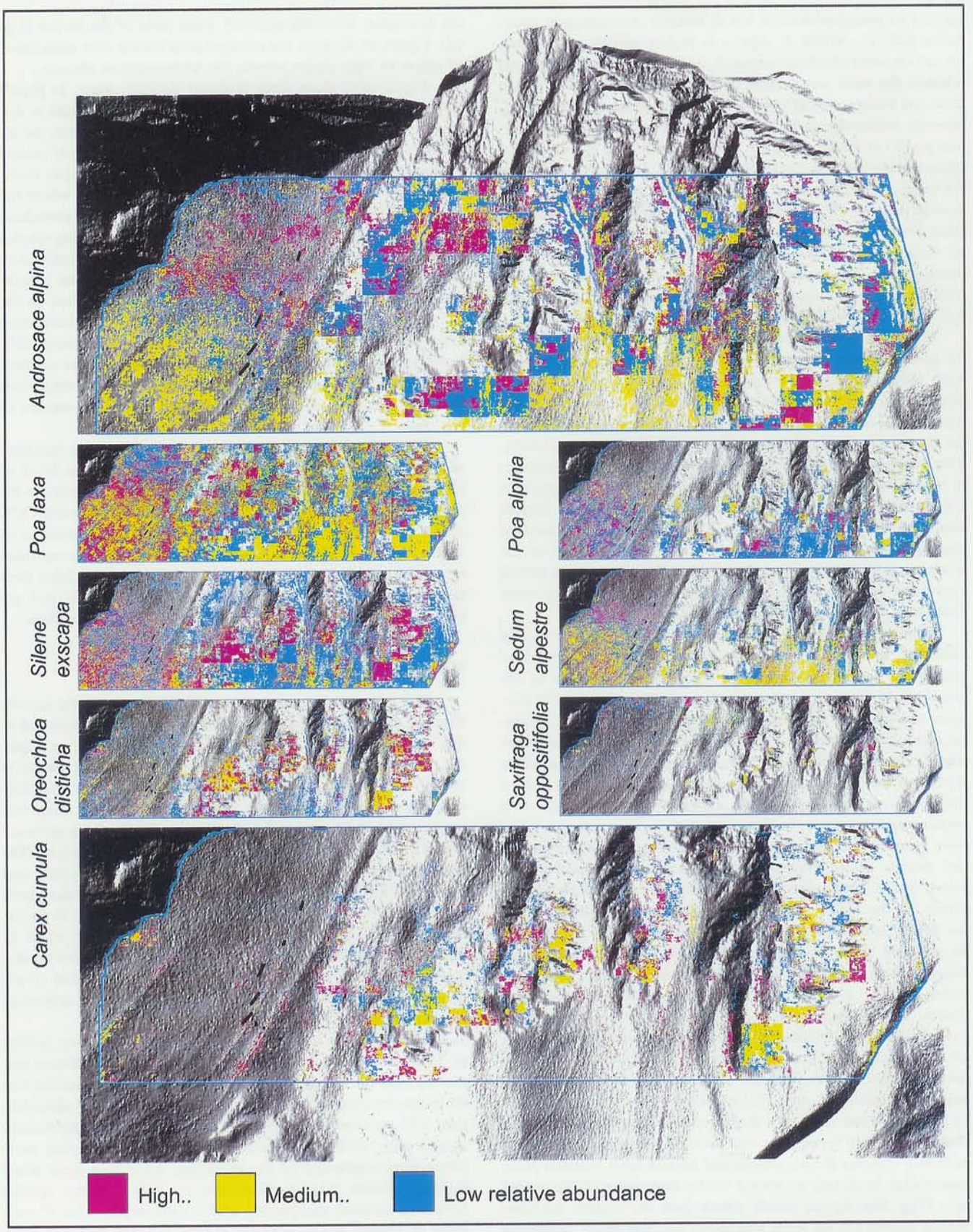

FIGURE 5. Predicted distributions of eight typical species, superimposed on the vertical view of the DEM. Black dots: sampled plots. Note that abundances are displayed not in absolute values, but relative to the highest sampled abundance of the respective species.

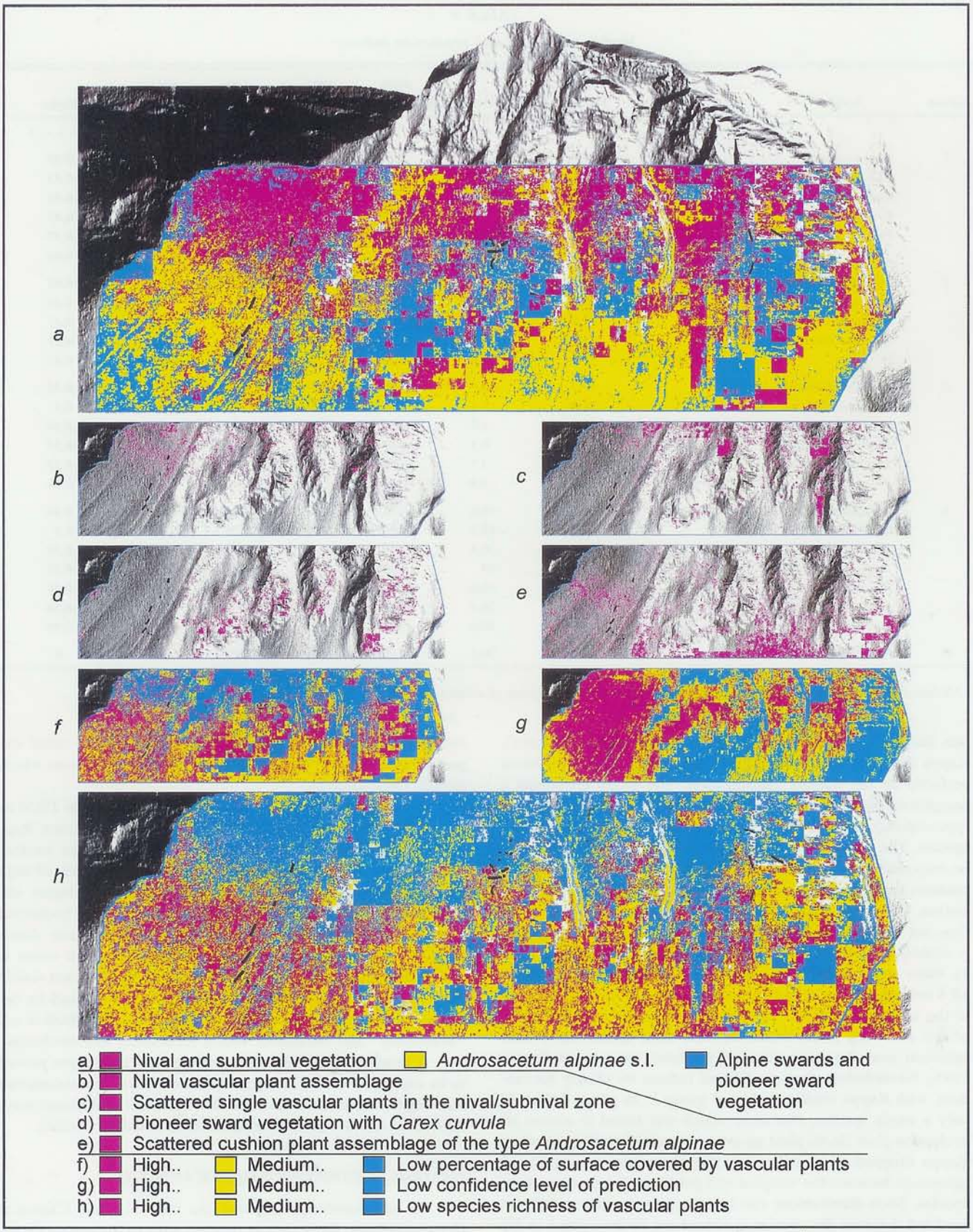

FIGURE 6. Predicted distributions of different types of vegetation (a–e)*, percentage of surface covered by vascular plants* (f)*, species richness* (h)*, and confidence level of the prediction* (g)*, superimposed on the vertical view of the DEM. Black dots: sampled plots.*

TABLE 4

Model evaluation and prediction indices[a]

Group	Species		s1-cases	s1p1-cases	s0p0-performance	s0p1-failure	s1p0-failure	s1p1-performance	Kappa
			n = 92	n = 92	%	%	%	%	0 < k < 1
1	*Carex curvula*		14.3	8.3	***109***	***38***	***49***	***477***	***0.55***
	Poa alpina		20.1	11.8	***114***	***40***	***51***	***320***	***0.53***
	Sedum alpestre		20.2	13.6	***116***	***51***	***42***	***279***	***0.52***
	Veronica alpina		11.2	6.7	***107***	***65***	***48***	***360***	***0.41***
	Festuca intercedens		17.3	9.6	***110***	***67***	***57***	***247***	***0.37***
		mean	16.6	10	111	52	49	337	0.48
2	*Oreochloa disticha*		27.1	17.1	***119***	***56***	***54***	***205***	***0.45***
	Androsace alpina		30	19.2	***122***	***61***	***56***	***180***	***0.41***
	Luzula spicata		51.7	38.6	***154***	***59***	***57***	***132***	***0.41***
	Gentiana bavarica		34.8	20.3	***122***	***61***	***64***	***165***	***0.37***
		mean	35.9	23.8	129	59	58	171	0.41
3	*Primula glutinosa*		33.7	18.6	***118***	***68***	***69***	***157***	***0.31***
	Erigeron uniflorus		22.8	11.6	***111***	***71***	***67***	***189***	***0.3***
	Saxifraga oppositifolia		11.2	4.7	***104***	***74***	***68***	***296***	***0.28***
	Minuartia gerardii		12.6	6.3	***106***	***79***	***63***	***234***	***0.27***
	Saxifraga exarata		18.2	7.7	***106***	***78***	***74***	***190***	***0.23***
		mean	19.7	9.8	109	74	68	213	0.28
4	*Cerastium uniflorum*		56.5	41.6	***155***	***65***	***66***	***122***	***0.34***
	Saxifraga bryoides		67.5	53.9	***180***	***68***	***70***	***112***	***0.3***
	Silene exscapa		43.6	30.4	***130***	***76***	***66***	***127***	***0.28***
	Tanacetum alpinum		64.6	49	***158***	***72***	***74***	***113***	***0.27***
	Ranunculus glacialis		56.9	41.6	***145***	***74***	***73***	***116***	***0.26***
	Minuartia sedoides		43.9	26.9	***124***	***73***	***74***	***129***	***0.26***
		mean	55.5	40.6	149	71	71	120	0.29
5	*Poa laxa*		80	70.6	***80***	***102***	***102***	***100***	0

[a] Values in bold italic were used for grouping the species. For explanation of columns see text.

tion failures (74% and 68% of the expected random failures), Kappa dropped. Interestingly, this group was reflected almost perfectly by the floristic classification. The group represents a basiphilous pioneer vegetation, characterized by *E. uniflorus, S. oppositifolia, M. gerardii,* and *S. exarata,* among a few other species. The somewhat ruderal character of this vegetation may be responsible for the high rate of prediction failures. Group 4 contains the ubiquitous species of the high alpine and nival vegetation. They were found in about 60% of the plots, being, therefore, not very precise to characterize concerning their topographic niches. Note that also in the CCA ordination diagrams (Fig. 4), these species formed a group positioned near the center of all 4 ordination axes, which indicates that they react indifferently to the involved gradients (a second, but unlikely interpretation of this centering effect would be, that these species have their optimum near the mean of each gradient; see e.g. ter Braak, 1995). Nevertheless, their predictions indices are clearly not random, with Kappa similar to that of group 3. In group 5 there is only a single species, *Poa laxa,* which was found in almost all evaluation plots (in 80 plots on average over 10 evaluation runs). Kappa dropped to 0, indicating that there was no significant agreement between the sampled and predicted distribution of the species. Such distributions can in principle not successfully be modeled, because the species is almost not differentiated in the sample set, at least according to its presence/absence.

Discussion

TERRAIN AND VEGETATION DISTRIBUTION PATTERNS

The initial hypothesis that distribution patterns of species and vegetation units at the alpine-nival ecotone can be explained using topographic descriptors holds. Obviously the relief expresses a remarkable part of the environmental conditions which control these patterns.

We used exclusively information derived from the DEM as the environmental descriptor set for the following reasons: Regular grid networks of climatic data, extrapolated from weather stations, still do not meet the resolution requirements of high alpine distribution modeling, whereas information layers obtained from aerial images are fine-scaled enough. The traditional information derived from such photographs have some disadvantages in high alpine environments: e.g., the snow cover is season dependent; vegetation or soil patterns are often not visible on a feasible photographic scale. Surface elevation and its derivatives, however, represent the only type of data which is not "seasonally" and obtainable with a sufficiently fine resolution.

A number of different topographic descriptor types proved to be especially useful in the analysis. Moreover, the assumption that vegetation patterns are related to the relief in different ways depending on the spatial resolution used could be verified.

CANONICAL CORRESPONDENCE ANALYSIS

To our knowledge this was the first time that Canonical Correspondence Analysis was coupled with a GIS system to perform spatial explicit predictive modeling. This combination, GIS as preprocessing tool for the spatial environmental analysis, CCA as prediction method, and GIS, again, as extrapolation machine and visualization platform, proved to be very useful.

CCA was criticized for its basic assumption of Gaussian response curves of species to environmental gradients (Austin et

al., 1994b), and alternative regression methods, for instance, Generalized Linear Modeling (McCullagh and Nelder, 1989; Nicholls, 1989, 1991), were suggested for gradient analyses. Although the Gaussian nature of species responses in this data set was not examined in detail, CCA proved to be an effective tool to describe the relations of vegetation to the relief, and the meaningful results obtained in this study justify its use.

From our viewpoint, CCA rewards the drawback of treating all species with the same response model (Austin et al., 1994b) with a clear advantage. While methods which model single species responses separately loose the information about the composition of species within samples, CCA uses exactly this information through its weighted averaging algorithm. Therefore, not only the position of species, but also of samples in relation to gradients can be defined. We used exactly this property by not predicting the occurrence of a particular species on a given point, but the occurrence of a particular vegetation sample. Species distribution patterns were obtained indirectly by extracting them from predicted sample distributions. In this sense the model can be seen as a vegetation-site model (Brzeziecki et al., 1993).

By defining the position of each modeled cell in the multidimensional CCA ordination space and assigning to it the vegetation of the nearest neighbor sampled in the field (based on Euclidean distance in the CCA space), it was guaranteed that only real existing species compositions could be predicted. Analyzing the responses of each species separately, predicting species distributions, and assembling predicted species compositions on new locations from them would probably create artificial vegetations not existing in reality. Especially when syntaxonomical units are under consideration, methods treating species separately should therefore be avoided.

Moreover, the proposed prediction method has the advantage that any information related to samples, e.g., assignments to vegetation types, species numbers, or cover values, can also be spatially extrapolated.

CONFIDENCE LEVEL OF PREDICTION AND MODEL EVALUATION

The constraints in the sampling design of the vegetation input data, which prevented a stratified random sampling, caused clear drawbacks. This can be demonstrated by inspecting Figure 6g. The confidence level of the prediction is high (magenta) near the sampled permanent plots and also on the broad southwest-exposed slope, where the terrain situation is very similar to that of the plots located in this part of the model area. The results are less reliable in the wide downslope scree areas, indicated by cyan pixels. Obviously, this topographic situation was not sampled sufficiently in the field, and, therefore, the power of the predictions for these areas, concerning for instance Figure 5, *P. alpina* and *S. alpestre,* is low. Nevertheless, these predictions are ecologically meaningful, which is supported by personal field observations of, for instance, *Poa alpina,* a frequent species on the downslope debris cones.

The problem continues in the model evaluation. Although good evaluation values were obtained, these measures came from sampled plots, and therefore are valid, in a strict sense, only within the areas of a high prediction confidence level, where the plots are lumped. An evaluation based on randomly selected control plots is planned for summer of 1998.

Conclusions

The strong interdependencies between the vegetation distribution patterns and the terrain conditions, which modify climate effects, highlight the vulnerability of the alpine-nival ecotone. Even small-scaled migration effects are likely to cause fundamental changes in species compositions of its vegetation units, which have well-defined and in some cases spatially limited niches. These impacts on mountain biodiversity are particularly severe when considering the endemic character of the zonal vegetation types of the Alps (Grabherr, 1995).

Mountain hydrology is likely to change with displacements along the ecotone. The strong variability over short distances of plant cover, and, hence, soil and area stabilized by roots, as shown by the presented patterns, expresses the hydrological sensibility of this high mountain zone.

Through its sensitiveness, the alpine-nival ecotone can be seen as an excellent potential sensor of the effects of climate change. Until monitoring results will be available, fine-scaled spatial modeling can help to generate hypotheses and future scenarios. Coupling the static model presented here with dynamical approaches (Monserud and Leemans, 1992) could be a promising tool coping with both the space and time dimension of the expected events.

Acknowledgments

We are grateful to Karl Reiter, who introduced us to GIS and DEMs, to Reinfried Mansberger and Werner Schneider, who produced the basic DEM, to Franz Michael Grünweis, who helped us with the facility management, and to all friends who supported us in the field. Many thanks to Stefan Boresch, Alan Brown, and Marc Yeo for their useful remarks on the manuscript. The study was financed by the Austrian Academy of Science (within the frame of the International Geosphere Biosphere Program) and the Austrian Federal Ministry of Science.

References Cited

Adams, J. M., Faure, H., Faure-Denard, L., McGlade, J. M., and Woodward, F. I., 1990: Increases in terrestrial carbon storage from the last glacial maximum to the present. *Nature,* 348: 711–714.

Auer, I., Böhm, R., and Mohnl, H., 1993: Die hochalpinen Klimaschwankungen der letzten 105 Jahre beschrieben durch Zeitreihenanalysen der auf dem Sonnblick gemessenen Klimaelemente. *Jahresbericht des Sonnblickvereins,* 88–89 (1990–1991): 3–36.

Austin, M. P., Meyers, J. A., and Doherty, M. D., 1994a: Predictive models for landscape patterns and processes. Modelling of landscape patterns and processes using biological data (Sub-project 2). Division of Wildlife and Ecology, Commonwealth Scientific and Industrial Research Organisation, Canberra. 44 pp.

Austin, M. P., Nicholls, A. O., Doherty, M. D., and Meyers, J. A., 1994b: Determining species response functions to an environmental gradient by means of a β-function. *Journal of Vegetation Science,* 5: 215–228.

Barry, R. G., 1992: *Mountain Weather and Climate.* London: Routledge. 402 pp.

Beerling, D. J., Huntley, B., and Bailey, J. P., 1995: Climate and the distribution of *Fallopia japonica*: use of an introduced species to test the predictive capacity of response surfaces. *Journal of Vegetation Science,* 6: 269–282.

Beniston, M., 1994: Climate scenarios for mountain regions. *In* Beniston, M. (ed.), *Mountain Environments in Changing Climates.* London: Routledge, 136–152.

Birks, H. J. B., Peglar, S. M., and Austin, H. A., 1994: An Annotated Bibliography of Canonical Correspondence Analysis and Related Constrained Ordination Methods 1986–1993. Botanical Institute, University of Bergen, Norway. 61 pp.

Böhm, R., 1993: Air temperature fluctuations in Austria 1775–1991—A contribution to greenhouse warming discussion. Preprints of the Eighth Conference on Applied Climatology, Jan. 17–22, 1993, Anaheim, CA: J26–J30.

Bonan, G. B. and Korzuhin, D., 1989: Simulation of moss and tree dynamics in the boreal forests of interior Alaska. *Vegetatio,* 84: 31–44.

Botkin, D. B., 1993: *Forest Dynamics: An Ecological Model.* Oxford: Oxford University Press. 309 pp.

Botkin, D. B., Janak, J. F., and Wallis, J. R., 1972: Some consequences of a computer model of forest growth. *Journal of Ecology,* 60: 849–873.

Box, E. O., 1981: *Macroclimate and Plant Forms: An Introduction to Predictive Modeling in Phytogeography.* The Hague: Junk. 258 pp.

Braun-Blanquet, J., 1964: *Pflanzensoziologie.* Vienna: Springer. 865 pp.

Brzeziecki, B., Kienast, F., and Wildi, O., 1993: A simulated map of the potential natural forest vegetation of Switzerland. *Journal of Vegetation Science,* 4: 499–508.

Brzeziecki, B., Kienast, F., and Wildi, O., 1995: Modelling potential impacts of climate change on the spatial distribution of zonal forest communities in Switzerland. *Journal of Vegetation Science,* 6: 257–268.

Bugmann, H. K. and Fischlin, A., 1992: Ecological processes in forest gap models—analysis and improvement. *In* Teller, A., Mathy, P., and Jeffers, J. N. R. (eds.), *Responses of Forest Ecosystems to Environmental Changes.* London: Elsevier Applied Science, 953–954.

Burton, P. J. and Urban, D. L., 1989: Enhanced simulation of early secondary forest succession by incorporation multiple life form interaction and dispersal. *In* Sjögren, E. (ed.), *Forests of the World, Diversity and Dynamics* (Abstracts), Studies in Plant Ecology, 18. Uppsala, Sweden: Svenska Växtgeografiska Sällskapet.

Coffin, D. P. and Lauenroth, W. K., 1990: A gap dynamics simulation model of succession in a semiarid grassland. *Ecological Modeling,* 49: 229–266.

Cohen, J., 1960: A coefficient of agreement for nominal scales. *Educational and Psychological Measurements,* 20: 37–46.

Cramer, W. P. and Leemans, R., 1993: Assessing Impacts of Climate Change on Vegetation Using Climate Classification Systems. *In* Solomon, A. M. and Shugart, H. H. (eds.), *Vegetation Dynamics and Global Change.* New York: Chapman and Hall, 190–217.

Emanuel, W. R., Shugart, H. H., and Stevenson, M. P., 1985: Climate change and the broad-scale distribution of terrestrial ecosystem complexes. *Climatic Change,* 7: 29–43.

ESRI 1995: ARC/INFO. Environmental Systems Research Institute, Inc., 1982–1995. Version 7.0.3.

Fulton, M. R., 1993: Rapid Simulations of Vegetation Stand Dynamics with Mixed Life-Forms. *In* Solomon, A. M. and Shugart, H. H. (eds.), *Vegetation Dynamics and Global Change.* New York: Chapman and Hall, 251–271.

Gauch, H. G., 1982: *Multivariate Analysis in Community Ecology.* Cambridge Studies in Ecology. Cambridge: Cambridge University Press. 298 pp.

Gottfried, M., Pauli, H., and Grabherr, G., 1994: Die Alpen im "Treibhaus": Nachweise für das erwärmungsbedingte Höhersteigen der alpinen und nivalen Vegetation. *Jahrbuch des Vereins zum Schutz der Bergwelt* (Munich), 59: 13–27.

Grabherr, G., 1995: Alpine vegetation in a global perspective. *In* Box, E. O., Peet, R. K., Masuzawa, T., Yamada, I., Fujiwara, K., and Maycock, P. F. (eds.), *Vegetation Science in Forestry.* Dordrecht: Kluwer Academic Publishers, 441–451.

Grabherr, G., Gottfried, M., Gruber, A., and Pauli, H., 1995: Patterns and current changes in alpine plant diversity. *In* Chapin, F. S., III and Körner, C. (eds.), *Arctic and Alpine Biodiversity: Patterns, Causes and Ecosystem Consequences.* Ecological Studies 113. Berlin: Springer, 167–181.

Grabherr, G., Gottfried, M., and Pauli, H., 1994: Climate effects on mountain plants. *Nature,* 369: 448.

Hill, M. O., 1979: TWINSPAN—a FORTRAN program for arranging multivariate data in an ordered two-way table by classification of individuals and attributes. Cornell University, Ithaca, N.Y.

Holdridge, L. R., 1947: Determination of world plant formations from simple climatic data. *Science,* 105: 267–268.

Houghton, J. T., Meiro Filho, L. G., Callander, B. A., Kattenberg, A., and Maskell, K. (eds.), 1996: *Climate Change 1995—The Science of Climate Change. Contribution of Working group I to the Second Assessment Report of the Intergovernmental Panel on Climate Change.* Cambridge: Cambridge University Press. 572 pp.

Humphries, H. C., Coffin, D. P., and Lauenroth, W. K., 1996: An individual-based model of alpine plant distribution. *Ecological Modelling,* 84: 99–126.

Kienast, F., 1987: FORECE—A Forest Succession Model for Southern Central Europe. Oak Ridge National Laboratory, Oak Ridge, Tennessee, ORNL/TM-10575.

Körner, Ch., 1995a: Impact of atmospheric changes on alpine vegetation: the ecophysiological perspective. *In* Guisan, A., Holten, J. I., Spichiger, R., and Tessier, L. (eds.), *Potential Ecological Impacts of Climate Change in the Alps and Fennoscandian Mountains.* Geneva: Editions des Conservatoire et Jardin botaniques, 113–120.

Körner, Ch., 1995b: Alpine plant diversity: A global survey and functional interpretations. *In* Chapin, F. S., III and Körner, C. (eds.), *Arctic and Alpine Biodiversity: Patterns, Causes and Ecosystem Consequences.* Berlin: Springer, 45–62.

Körner, Ch. and Larcher, W., 1988: Plant life in cold climates. *In* Long, S. F. and Woodward, F. I. (eds.), *Plant and Temperature.* Cambridge: Company of Biologists, 25–57.

Larcher, W., 1994: *Ökophysiologie der Pflanzen.* Stuttgart: Ulmer. 394 pp.

Leemans, R., 1989: Possible changes in natural vegetation patterns due to a global warming. *In* Hackl, A. (ed.), *Der Treibhauseffekt: das Problem—Mögliche Folgen—Erforderliche Massnahmen.* Laxenburg, Austria: Akademie für Umwelt und Energie, 105–122.

Leemans, R. and Cramer, W., 1990: The IIASA climate database for land areas on a grid with 0.5° resolution. WP-90-41. Laxenburg, Austria: International Institute for Applied Systems Analysis.

Lenihan, J. M., 1993: Ecological response surfaces for North American boreal tree species and their use in forest classification. *Journal of Vegetation Science,* 4: 667–680.

Martin, Ph., 1993: Vegetation responses and feedbacks to climate: a review of models and processes. *Climate Dynamics,* 8: 201–210.

McCullagh, P. and Nelder, J. A., 1989: *Generalized Linear Models.* London: Chapman and Hall. 511 pp.

Mitchell, P. L., 1994: Climate and vegetation change. The influence of changes in climate and carbon dioxide on biome distribution. Interim report of the consortium led by Professor F. I. Woodward. Project 3b of Tiger IV. Sheffield: Archer Print. 23 pp.

Monserud, R. A. and Leemans, R., 1992: Comparing global vegetation maps with the Kappa Statistic. *Ecological Modelling,* 62: 275–293.

Montgomery, D. C. and Peck, E. A., 1982: *Introduction to Linear Regression Analysis.* New York: Wiley. 504 pp.

Moore, I. D., Grayson, R. B., and Ladson, A. R., 1991: Digital Terrain Modelling: A Review of Hydrological, Geomorphological, and Biological Applications. *Hydrological Processes,* 5: 3–30.

Moser, W., 1973: Licht, Temperatur und Photosynthese an der Station "Hoher Nebelkogel" (3184 m). *In* Ellenberg, H. (ed.), *Ökosystemforschung.* Berlin: Springer, 203–223.

Moser, W., Brzoska, W., Zachhuber, K., and Larcher, W., 1978:

Ergebnisse des IBP-Projekts "Hoher Nebelkogel 3184 m". *Sitzungsberichte der Mathematisch-Naturwissenschaftlichen Klasse,* Innsbruck. 387–419.

Nicholls, A. O., 1989: How to make biological surveys go further with generalized linear models. *Biological Conservation,* 50: 51–76.

Nicholls, A. O., 1991: Examples of the use of generalized linear models in analysis survey data for conservation evaluation. *In* Margules, C. R. and Austin, M. P. (eds.), *Nature Conservation: Cost Effective Biological Surveys and Data Analysis.* Melbourne: CSIRO, 191–201.

Ozenda, P., 1985: *La végétation de la Chaine alpine dans l'ensemble montagnard européen.* Paris: Masson. 344 pp.

Ozenda, P. and Borel, J.-L., 1991: *Mögliche Auswirkungen von Klimaveränderungen in den Alpen.* Internationale Alpenschutz-Kommission CIPRA, Kleine Schriften 8/91. 71 pp.

Pastor, J. and Post, W. M., 1985: Development of a linked forest productivity-soil process model. ORNL/TM-9519. Environmental Sciences Division Publication 2455, Oak Ridge National laboratory.

Pauli, H., Gottfried, M., and Grabherr, G., 1996: Effects of climate change on mountain ecosystems—upward shifting of alpine plants. *World Resource Review,* 8: 382–390.

Pauli, H., Gottfried, M., Reiter, K., and Grabherr, G., 1998: Monitoring der floristischen Zusammensetzung hochalpin/nivaler Pflanzengesellschaften. *In* Traxler, A. (ed.), *Handbuch des Vegetationsökologischen Monitorings.* UBA-Monographien, 89, A, B. Vienna: Umweltbundesamt (in press).

Peters, R. L. and Darling, J. D. S., 1985: The greenhouse effect and nature reserves: global warming would diminish biological diversity by causing extinctions among reserve species. *Bioscience,* 35: 707–717.

Prentice, I. C., 1986: The design of a forest succession model. *In* Fanta, J. (ed.), *Forest Dynamics Research in Western and Central Europe.* Wageningen, Netherlands: PUDOC, 253–256.

Prentice, I. C., van Tongeren, O., and de Smidt, J. T., 1987: Simulation of heathland vegetation dynamics. *Journal of Ecology,* 75: 203–219.

Prentice, I. C., Webb, R. S., Ter-Mikhaelian, M. T., Solomon, A. M., Smith, T. M., Pitovranov, S. E., Nikolov, N. T., Minin, A. A., Leemans, R., Lavorel, S., Korzukhin, M. D., Helmisaari, H. O., Hrabovszky, J. P., Harrison, S. P., Emanuel, W. R., and Bonan, G. B., 1989: Developing a global vegetation dynamics model: results of an IIASA summer workshop. Research Report RR-89-7, International Institute for Applied System Analysis, Laxenburg, Austria. 48 pp.

Reisigl, H. and Pitschmann, H., 1958: Obere Grenzen von Flora und Vegetation in der Nivalstufe der zentralen Ötztaler Alpen (Tirol). *Vegetatio,* 8: 93–129.

Schimper, A. F. W., 1898: *Pflanzengeographie auf physiologischer Grundlage.* Jena: Fischer. 876 pp.

Shugart, H. H., 1984: *A Theory of Forest Dynamics.* New York: Springer. 278 pp.

ter Braak, C. J. F., 1986: Canonical correspondence analysis: a new eigenvector technique for multivariate direct gradient analysis. *Ecology,* 67: 1167–1179.

ter Braak, C. J. F., 1988: CANOCO—a FORTRAN program for canonical community ordination by (partial) (detrended) (canonical) correspondence analysis, principal components analysis and redundancy analysis (version 2.1). Technical Report LWA-88-02, GLW, Wageningen. 95 pp.

ter Braak, C. J. F., 1990: Update Notes: Canoco Version 3.10. Agricultural Mathematics group, Wageningen. 35 pp.

ter Braak, C. J. F., 1995: Ordination. *In* Jongman, R. H. G., ter Braak, C. J. F., and van Tongeren, O. F. R. (eds.), *Data Analysis in Community and Landscape Ecology.* Cambridge: Cambridge University Press, 91–169.

ter Braak, C. J. F. and Looman, C. W. N., 1995: Regression. *In* Jongman, R. H. G., ter Braak, C. J. F., and van Tongeren, O. F. R. (eds.), *Data Analysis in Community and Landscape Ecology.* Cambridge: Cambridge University Press, 29–72.

Walter, H., 1985: *Vegetation of the Earth and Ecological Systems of the Geo-biosphere.* Berlin: Springer. 318 pp.

Woodward, F. I., Smith, T. M., and Emanuel, W. R., 1995: A global land primary productivity and phytogeography model. *Global Biochemical Cycles,* 9: 471–490.

Ms submitted September 1997